PNAS
www.pnas.org

Supplementary Information for

Immunization with lytic polysaccharide monooxygenase CbpD induces protective immunity against *Pseudomonas aeruginosa* pneumonia

Fatemeh Askarian[a,1], Chih-Ming Tsai[a], Gabriele Cordara[b], Raymond H. Zurich[a], Elisabet Bjånes[a], Ole Golten[c], Henrik Vinther Sørensen[b], Armin Kousha[a], Angela Meier[d], Elvis Chikwati[e], Jack-Ansgar Bruun[f], Judith Anita Ludviksen[g], Biswa Choudhury[h], Desmond Trieu[a,i], Stanley Davis[a], Per Kristian Thorén Edvardsen[c], Tom Eirik Mollnes[g,j,k], George Y. Liu[a], Ute Krengel[b], Douglas J. Conrad[l], Gustav Vaaje-Kolstad[c], Victor Nizet[a,h,m,1*]

[a]Division of Host-Microbe Systems & Therapeutics, Department of Pediatrics, University of California San Diego, La Jolla, CA 92093. [b]Department of Chemistry, University of Oslo, N-0315 Oslo, Norway. [c]Faculty of Chemistry, Biotechnology and Food Science, Norwegian University of Life Sciences, N-1432 Ås, Norway. [d]Division of Critical Care, Department of Anesthesiology, University of California San Diego, La Jolla, CA 92037. [e]Department of Paraclinical Sciences, Faculty of Veterinary Medicine, Norwegian University of Life Sciences, N-1432 Ås, Norway. [f]Proteomics and Metabolomics Core Facility, Department of Medical Biology, The Arctic University of Norway, N-9037 Tromsø, Norway. [g]Research Laboratory, Nordland Hospital, N-8005 Bodø, Norway. [h]Glycobiology Research and Training Center, UC San Diego, La Jolla, CA 92093. [i]School of Pharmacy, University of California San Francisco, San Francisco, CA 94143. [j]Department of Immunology, University of Oslo Hospital, N-0424 Oslo, Norway. [k]Center of Molecular Inflammation Research, Norwegian University of Science and Technology, N-7491 Trondheim, Norway. [l]Division of Pulmonary, Critical Care and Sleep Medicine, University of California San Dego, La Jolla, CA 92037. [m]Skaggs School of Pharmacy and Pharmaceutical Sciences, University of California San Diego, La Jolla, CA 92093.

[1]To whom correspondence should be addressed:
E-mail: vnizet@health.ucsd.edu , faaskarian@health.ucsd.edu
Tel: (+1) 858-534-7408, (+1) 858-534-9760

This PDF file includes:
Supplemental Materials and Methods
Supplemental Figures (including figure legends) S1-S6
Tables S1-S2
SI References
Description of additional supplemental files (Dataset Legends)

Other supplementary materials for this manuscript include the following:
Datasets 1-4

Supplemental Materials and Methods

Bacterial strains, constructs, cells, and serum collection

PA strains used in this study included WT PA14 (UCBPP-PA14 (1)), isogenic mutant PA14 Δ*cbpD* (ΔCbpD, provided by Prof. Deborah Hogan, Dartmouth). The trans-complemented constructs (ΔCbpD:CbpD and ΔCbpD:vector) were generated using the pGM931 vector (2) (provided by Prof Federica Briani, University of Milan) as previously described (3). Clinical CF patient strains $PA103_{UCSD}$ and $PA109_{UCSD}$ were provided by Dr. Ruth Siew (UC San Diego, UCSD), confirmed by PCR to harbor *cbpD* in their genome using primer set *cbpD*-FW: 5'-ATGAAACACTACTCAGCCACCCTGG-3' and *cbpD*-RV: 5'-TTACAGCAGGGTCCAGGCGTCCTGC-3'.

Recombinant CbpD variants including full-length rCbpD, AA10 (residues 1–210), and M2+CBM73 (residues 211–389) were constructed in the pNIC-CH vector (Addgene) using ligation-independent cloning and expressed in *Escherichia coli* BL21 Star (DE3, Invitrogen) as previously described (3). Recombinant full-length rCbpD (*cbpD* gene with its native promoter and C-terminal histidine tag) was constructed in pGM931 and expressed in the ΔCbpD strain as described (3). All recombinant constructs had a poly-histidine tag (His_6 tag) at the C-terminus of the protein. PA was propagated in Luria–Bertani broth (LB, BD Difco) at 37 °C and 200 rpm. When indicated (*growing* trans complemented constructs) carbenicillin and arabinose were supplemented to the growth media (3).

Human neutrophils were isolated from the freshly heparinized venous blood of healthy volunteers (see "Ethical approval") using 1-Step Polymorphprep (Fresenius Kabi Norge AS) gradient centrifugation. Murine alveolar macrophages (AMs) were cultured in RPMI 1640 (Gibco) containing L-glutamine (Gibco), supplemented with 10% (v/v) heat inactivated FBS (Gibco), 10 mM HEPES (Gibco), penicillin (100 units mL^{-1}), and 100 µg mL^{-1} streptomycin (Gibco), 4.5 g L^{-1} glucose (Gibco), 1.0 mM sodium pyruvate (Gibco) and 0.05 mM 2-mercaptoethanol (Sigma). The cells were maintained at 37 °C with 5% CO_2.

To prepare human serum or plasma, blood was drawn from multiple healthy volunteers (see "Ethical approval"), permitted to clot for 15 min at room temperature (RT) (if needed), followed by centrifugation (10 min, 2000 × *g*). Normal human serum (NHS)/plasma were pooled collected and stored at −70 °C. Heat-inactivated normal human serum (HI-NHS) was prepared by incubation in a 56 °C water bath for 30 min. Sera deficient for complement components and normal human serum (as control) were purchased from Complement Technology (Texas, USA). Human plasma from CF patients (see "Ethical approval") were collected from heparinized blood by centrifugation (15 min, 2000 × *g*) and stored at −70 °C.

Protein production and purification

The constructs that were used for expression and purification of His-tagged CbpD or truncated variants (AA10 and M2+CBM73) from *E. coli* BL21 Star (DE3) and *PA* (ΔCbpD) are described previously (3). Briefly, bacteria harboring the expression construct were grown in LB or Terrific Broth (TB) medium + 50 µg mL^{-1} kanamycin (*E. coli*) or 300 µg mL^{-1} carbenicillin (PA) at 37 °C and 220 rpm shaking. Upon reaching OD_{600nm} = 0.6 – 0.7, isopropyl-β-D-thiogalactoside (IPTG, Sigma) or arabinose (Sigma) were added to final concentrations = 0.50 – 1.0 mM (*E. coli*) or 6.6 mM (PA), respectively. Cultures were incubated overnight for 16 h at 22 – 25 °C in a LEX-24 Bioreactor (Harbinger Biotechnology) or a shaking incubator (220 rpm). Recombinant proteins were purified from the clarified periplasmic extracts (full-length CbpD and AA10 domain) or cytoplasmic lysate (M2+CBM73) using a HisTrap™ High-Performance column (GE Healthcare) connected to an ÄKTA Purifier FPLC system (GE Healthcare), as previously described (3) or His60 Ni Superflow Resin (Takara) chromatography per manufacturer's instructions. When applicable, impurities were eliminated using an ÄKTA purifier chromatography system equipped with a HiLoad 16/6016/600 Superdex 75 size-exclusion column (GE Healthcare). Proteins were kept 15 mM Tris-HCl pH 7.5/150 mM NaCl. When needed (e.g., for immunization) the buffer was exchanged to cell culture grade 1 x PBS (without Ca^{2+} and Mg^{2+}), using centrifugal concentrators with molecular weight cutoff of 10 kDa (Sartorius Stedim Biotech GmbH or ThermoFisher) and passed through a Pierce™ high-capacity endotoxin removal column (ThermoFisher). The concentration of the purified protein was estimated by Nanodrop (absorbance at A280) using the theoretical extinction coefficient.

Murine model of immunization

Mice (see "Ethical approval") were housed in filter-top cages with access to food pellets and water in conditions of controlled ambient temperature (20 – 22 °C) and relative humidity (30 – 70%), with a 12 h light/12 h dark cycle. Six-week-old female CD-1 mice (Charles River Laboratories) were intraperitoneally (IP) immunized three times with recombinant full length CbpD ($CbpD_{25}$: 25, 25, 25

μg/mouse; $CbpD_{75}$: 75, 50, 50 μg/mouse), AA10 (25, 25, 25 μg/mouse) and M2+CBM73 (25, 25, 25 μg/mouse) at seven-day intervals (as described in Fig. 3A). The recombinant purified protein was mixed with aluminium hydroxide (aluminum hydroxide gel, InvivoGen, vac-alu-250) (450 μg/mouse). Aluminium hydroxide alone, supplementing PBS, was included as a mock-immunization control mouse. Murine sera were collected using BD Microtainer to profile cytokines or anti-CbpD antibodies by ELISA.

Murine model of intratracheal (IT) PA infection

IT infection was performed as previously described (3). Overnight culture of PA was re-grown to exponential growth phase (OD_{600} = 0.50 – 0.60) at 37 °C and 200 rpm and washed with PBS. Depending on the PA strain, the pellet diluted in PBS to yield a final concentration of 2.5 – 5 × 10^6 CFU/30 μL/mouse for the survival curve assay, 0.5 – 2 × 10^6 CFU/30 μL/mouse for the bacterial burden assays, and 1 – 2 × 10^5/30 μL/mouse in the recurrent PA exposure model. Inocula were confirmed by serial dilution and CFU determination on LB agar plates. CD-1 mice (Charles River Laboratories, female, 8 to 11-week-old) and C57BL/6 (WT) and complement C3-deficient mice ($C3^{-/-}$) (Charles River Laboratories, 8 to 11-week-old, matched female, or male) were anesthetized with 100 mg kg^{-1} ketamine and 10 mg kg^{-1} xylazine. Next, the vocal cords were visualized with an operating otoscope (Welch Allyn) and bacteria (inoculation volume of 30 μL) administered intratracheally using a long, sterile pipette tip. Mice were placed on a warmed pad for recovery. For survival curve assays, mice were observed every 12 – 18 h after infection, and deaths were recorded accordingly. For bacterial burden assay, mice were euthanized 24 h post infection, and lung homogenized using a Mini BeadBeater 96 (BIOSPEC Products), serially diluted in PBS, plated on LB agar for CFU enumeration, and results reported as CFU/g lung tissue. Instilled CFU and mouse numbers per experiment are recorded in the figure legends. When indicated, mock-infected mice (PBS/30 μL per mouse) were included as a control. When applicable, murine sera and plasma were collected using BD Microtainer and/or BD Microtainer with K2E (K_2EDTA), respectively.

Lung histopathology analysis

Lungs of the infected (WT and ΔCbpD) or mock-infected animals (n = 5 mice/group) were fixed in 10% (v/v) paraformaldehyde (PFA) for 24 h, followed by incubation in 70% ethanol for long-term storage. Tissue sectioning and staining were performed at the UC San Diego Comparative Phenotyping Core. Briefly, lung sections were deparaffinized per established protocols by immersion in xylene, rehydration in an ethanol/water gradient, and washing with deionized (DI) water. For microscopy, rehydrated slides were stained with hematoxylin and eosin and images captured using an Olympus BX43 light microscope equipped with an IDS UI3260CP-C-HQ 2.3 MP camera (IDS Imaging Development Systems GmbH) and MicroVisioneer (MicroVisioneer Freising) whole slide scanning software.

Murine model of systemic PA infection

Systemic infection of CbpD- ($CbpD_{25}$ and $CbpD_{75}$ regimens) and mock-immunized 9-week-old female CD-1 mice (Charles River Laboratories) was performed as previously described (3). Overnight culture of WT PA was re-grown in LB to the exponential growth phase (OD_{600} = 0.4 – 0.5) at 37 °C and 200 rpm. PA were washed with PBS and the pellet diluted in PBS to a final concentration of 2 × 10^7 CFU/mouse. Mice were IV infected via tail vein. For survival curve assays, mice were observed every 12 h after infection and deaths recorded accordingly. For the bacterial burden assays, mice were euthanized 4 h post infection, and kidney, spleen, and blood (heparinized) were collected. The organs were homogenized using a Mini BeadBeater. Homogenized samples and heparinized blood were serially diluted in PBS and plated on LB agar for CFU enumeration reported as CFU/gr or CFU/mL; instilled CFU and mouse numbers are reported in the figure legends.

Isolation and infection of murine alveolar macrophages (AMs)

Alveolar macrophages were collected from bronchoalveolar lavage (BAL) of 10-week-old female CD-1 mice (Charles River Laboratories). Mice (n = 5 mice per experiment) were anesthetized with intraperitoneal administration of 200 mg kg^{-1} ketamine and 20 mg kg^{-1} xylazine. BAL was collected as previously described (4) with minor modifications. Approximately, 1 mL of pre-warmed PBS + 0.5 mM EDTA (Invitrogen) was gradually instilled into the lung. After a few seconds, BAL fluid was collected in 15 mL ice-cold canonical tubes. Cells were centrifuged (10 min, 400× *g*, 4 °C), resuspended in RPMI/FBS and seeded in 96-well plates at 5.5 – 6 × 10^4 per well. Media were replaced 24 h post-collection to remove non-adherent cells. At 48h post-collection, adherent AMs were washed with PBS and RPMI/FBS without antibiotics added to the cells. Overnight culture of WT and ΔCbpD were re-grown in LB to exponential growth phase (OD_{600} = 0.6 – 0.7) at 37 °C and 200 rpm. PA strains were washed with PBS, and the pellet diluted in antibiotic free $RPMI_{AMs}$. Bacterial cells were opsonized with

5% pooled murine sera for 2 min and the opsonized bacteria were added to the cells at multiplicity of infection (MOI)=10. The plate was centrifuged (5 min, 400× *g*, RT) and cells incubated at 37 °C (5% CO_2) for 1.5, washed with PBS, and lysed with 1% (v/v) Triton x-100 (Sigma). Bacterial survival was evaluated by serial dilution in PBS with subsequent plating on LB agar plates, followed by overnight incubation at 37 °C and counting of colonies.

Fluorescence microscopy analysis of AMs
AMs were seeded in 8-well cell culture chamber slides (Nunc) at a density of 1.5×10^5 cells/well. Cells were fixed by incubation with 4% paraformaldehyde (v/v) for 20 min at RT, permeabilized with 0.3% (v/v) Tween-20 (Sigma) (3 min, RT), and blocked with 10% (v/v) FBS (2 h, RT). Thereafter, cells were immune-stained using PE Rat Anti-Mouse Siglec-F (Clone E50-2440, BD Bioscience, 10 µg/mL) or FITC hamster anti-mouse CD11c (Clone HL3, BD Bioscience, 10 µg/mL) and 4',6-diamidino-2-phenylindole (DAPI, Invitrogen, dilution 1:500). Imaging was performed by the Zeiss AxioObserver D1 microscope (Zeiss, Germany).

Serum killing assay
Overnight cultures of WT or ΔCbpD PA were re-grown in LB to exponential growth phase (OD_{600} = 0.60 – 0.70) at 37 °C and 200 rpm. PA strains were washed with PBS, the pellet resuspended in RPMI at OD_{600} = 0.40, and the bacterial culture diluted further in RPMI (10X). Next, 160 µL of RPMI, 20 µL of pooled NHS (final concentration 10%), HI-NHS or complement deficient sera and 20 µL of 10X diluted bacterial stock were added to a low-binding Eppendorf tube and incubated for 1 h at 37 °C on a shaker. Bacterial survival was evaluated by serial dilution in PBS with subsequent plating on LB agar plates, followed by overnight incubation at 37 °C and counting of colonies.

Neutrophil killing assay
WT, ΔCbpD, $PA109_{UCSD}$, and $PA103_{UCSD}$ cultures were prepared as described in "Serum killing assay". The bacteria were washed with PBS and resuspended in RPMI at the desired CFU. PA strains were opsonized with 5% pooled NHS for 2 min or 5% murine sera for at least 5 min at 37 °C on a shaker using low-binding Eppendorf tubes or 96-well round bottom. Next, the opsonized bacteria were added to freshly purified human neutrophils ($5x10^5$) at the indicated MOI and incubated for 30 min at 37 °C on a shaker or horizontal rotator. The cells were lysed with ice-cold H_2O supplemented with 0.3% saponin. Bacterial survival was evaluated by serial dilution in PBS with subsequent plating on LB agar plates, followed by overnight incubation at 37 °C and counting of colonies.

CbpD-specific antibody response in human and murine sera
CbpD-specific antibody titers in human and murine sera were measured by ELISA. Briefly, high binding microtiter plates (Corning) were coated with 1 µg/well recombinant CbpD variants (full length, AA10 or M2+CBM73) in PBS and incubated overnight at 4 °C. Wells were blocked with 1% (w/v) bovine serum albumin (BSA, Sigma) for 2 h at RT followed by washing with PBS supplemented with 0.05% (v/v) Tween 20 (Sigma). Serially diluted sera (100 µl) in PBS were added to the wells and incubated for 2h at RT. Bound antibodies were detected by HRP-conjugated goat anti-mouse IgG (clone: Poly4053, BioLegend # 405306, dilution: 1:5000) or HRP-conjugated donkey anti-human IgG (clone: 24109, Biolegend # 410902, dilution 1:5000) using TMB substrate set (OptEIA™). A Multimode Plate Reader was used to measure absorbance at 450 nm.

Cytokine profiling in murine sera or organ homogenates
Murine sera and organ homogenates (lung and spleen) were analyzed using the Bio-Plex Pro™ Mouse Cytokine 23-plex Assay (Bio-Rad) per manufacturer's instructions. Murine sera were collected from freshly drawn blood in BD Microtainer serum separator tubes (10 min, 10000 × *g*, 4 °C) by centrifugation and stored at -70 °C. Organ homogenates were prepared using a Mini BeadBeater 96 followed by centrifugation (10 min, 10000 × *g*, 4 °C) and stored at -70 °C.

Complement analysis (C3b-assay)
Murine plasma was collected from freshly drawn blood using BD Microtainer tubes with K2E (K_2EDTA) by centrifugation and stored at -70 °C. Plasma was used to measure C3 activation (C3b-assay, Hycult Biotech, Uden, The Netherlands) per manufacturer's instructions. The C3b assay detects an activation epitope present on C3b, iC3b and C3c, but not in native C3, thus specifically indicates activation of C3.

***In vivo* depletion of neutrophils**

Eight-week-old naïve CD-1 mice were intraperitoneally treated with anti-mouse Ly6G (clone 1A8, Bio X Cell # BE0075-1, 100 µg/mouse) or corresponding isotype control (clone 2A3, Bio X Cell # BE0089, 100 µg/mouse) (5). To confirm depletion, spleens (n = 3 mice per group) were collected, processed for single-cell isolation, and stained with LIVE/DEAD™ fixable aqua dead Cell Stain Kit (Invitrogen # L34957), FITC rat anti-mouse CD19 (clone: 1D3, BD Bioesciences # 557398, 0.1 µg per $1x10^6$ cells in 1 mL volume), Alexa Fluor® anti-mouse CD3 (clone: 17A2, BioLegend # 100210, 1 µg per $1x10^6$ cells in 1 mL volume), pacific blue™ CD11b monoclonal antibody (M1/70.15, Invitrogen # RM2828, 0.1 µg per $1x10^6$ cells in 1 mL volume), PE/Cyanine7 anti-mouse Ly-6C (clone: HK1.4, BioLegend # 128018, 0.6 µg per $1x10^6$ cells in 1 mL volume), APC anti-mouse Ly-6G (clone: 1A8, BioLegend # 127614, 0.6 µg per $1x10^6$ cells in 1 mL volume). Stained splenocytes were analyzed by flow cytometry using FACSCanto II (BD Bioscience) and FlowJo software. Mice were intratracheally infected with $0.1x10^6$ CFU/30 µL/mouse as described in "Murine model of intratracheal (IT) PA infection". Mice were observed every 12 h after infection, and lethal events recorded. Mouse numbers are depicted in the figure legends.

***In vivo* depletion of CD4 cells**

CbpD- ($CbpD_{75}$ regimen)- and mock-immunized nine-week-old female CD-1 (immunized as described in "murine model of immunization") were IV treated with two doses of Ultra-LEAF™ purified anti-mouse CD4 antibody (clone: GK1.5, BioLegend # 100457, 300 µg/mouse) or Ultra-LEAF™ purified rat IgG2b, κ isotype control (clone: RTK4530, BioLegend#400671, 300 µg/mouse) on day 2 and day 1 prior to IT infection ($1x10^6$ CFU/30 µL/mouse). To confirm depletion, spleens (n = 2 mice per group) were collected, processed for single-cell isolation, and stained with Zombie Violet viability dye (Biolegend # 423113), Alexa Fluor® 488 anti-mouse CD3 (clone: 17A2, BioLegend # 100210, 1 µg per $1x10^6$ cells in 100 µL volume), APC anti-mouse CD4 (clone: RM4-4, BioLegend # 116014, 0.2 µg per $1x10^6$ cells in 100 µL volume) and PE anti-mouse CD8a Antibody (clone: 53-6.7, BioLegend # 100708, 0.2 µg per $1x10^6$ cells in 100 µL volume). Stained splenocytes were analyzed by flow cytometry using FACSCanto II (BD Bioscience) and FlowJo software. Next, 24 h after transfer of the final antibody dose, the mice were IT infected with WT PA ($1x10^6$ CFU/30 µL/mouse) as described above. Lungs were collected 24 h postinfection, homogenized, serially diluted in PBS, and plated on LB agar for CFU enumeration (CFU/gr). Mouse numbers and instilled CFU and mouse numbers are reported in the figure legends.

Adoptive transfer of anti-CbpD IgG *in vivo*

Serum was collected from CbpD immunized female CD-1 mice ($CbpD_{75}$) and anti-CbpD IgG affinity purified using Pierce™ NHS-Activated Agarose (ThermoFisher) by immobilization of 1 mg recombinant CbpD as instructed by the manufacturer's protocol. Next, the buffer of the purified CbpD-IgG was exchanged to cell culture 1xPBS (without calcium and magnesium) using centrifugal concentrators with the molecular weight cutoff of 100-kDa (ThermoFisher). Affinity purified anti-CbpD IgG, or mouse IgG (Sigma) was IV (retro-orbital) transferred to seven-week-old naïve female CD-1 mice at either single dose (70 µg/mouse) or two doses (200 and 100 µg/mouse, 16 h interval). Next, the mice were IT infected with $1x10^6$ or $2.5x10^6$ CFU/mouse WT PA 16 h after administration of the final antibody dose (as described above). Lungs were collected 24 h postinfection, homogenized, serially diluted in PBS, and plated on LB agar for CFU enumeration (CFU/gr); mouse numbers are reported in the figure legends.

CbpD-IgG neutralization assay

The activity of CbpD on β-chitin was determined using a previously described procedure with modifications (3). Purified rCbpD was saturated with a five-fold molar excess of copper (Cu(II)SO4) for 30 min at RT. Thereafter, the enzyme was passed through a PD MidiTrap G-25 column (GE Healthcare) for removal of the excess copper, and the buffer was exchanged to 15 mM Tris-HCl pH 7.5/150 mM NaCl. CbpD activity in the presence or absence of CbpD-IgG was assessed by incubating 2.5 $mg \cdot ml^{-1}$ β-chitin (France Chitin) with 1 µM of the protein in a total of 200 µl reaction that were buffered with 20 mM Tris-HCL pH 7.0 in the presence or absence of 1 mM ascorbate (Sigma). The samples were incubated at 37 °C for 3 h under shaking at 220 rpm. When indicated, copper saturated CbpD was incubated with CbpD-IgG (at the indicated concentrations) for 30 min at 4 °C under shaking before the reaction was started.

Reaction products were analyzed using a high-performance anion exchange chromatography pulsed amperometry detector (HPAEC-PAD) (ICS-3000, Dionex Thermo Scientific, Sunnyvale, USA) as described previously with modifications (6). A CarboPac PA-1 column (4 mm x 250 mm) attached to a CarboPac PA1-guard column (4mm x 50mm) was used, and data were acquired using manufacturer's supplied standard Quad waveform for carbohydrates. Solvent-A (100mM NaOH containing 7mM

sodium acetate) and solvent-B (100 mM NaOH plus 1M NaOAc) were used as elution solvents, at a flow rate of 1 mL/min for a total run time of 50 min. Details of the gradient condition were as follows: 0 min: solvent A (100%), solvent B (0); 10 min: solvent A (90%), solvent B (10%); 25 min: solvent A (70%), solvent B (30%); 30 min: solvent A (0%), solvent B (100%); 35 min: solvent A (0%), solvent B (100%); 37 min: solvent A (100%), solvent B (0%); 50 min: solvent A (100%), solvent B (0%). Aldonic acids obtained from the reactions were elute according to a mixture of chitooligosaccharide aldonic acids standards.

Flow cytometric analysis of CbpD antibody binding to PA cell surface

Overnight culture of PA was re-grown in LB to exponential growth phase (OD_{600} = 0.50 – 0.60) at 37 °C and 200 rpm, washed with PBS, and blocked in heat-inactivated horse serum (10% v/v, Sigma, H1138) at room temperature for 1 h. Murine sera were supplemented at a final concentration of 2% (v/v) and the samples were incubated at room temperature for 1 h. Bacteria were washed and incubated with Alexa Fluor™ 488 conjugated rabbit anti-mouse IgG (ThermoFisher, A-11059, 1:200). The samples were analyzed by FACSCanto II (BD Biosciences) and FlowJo software. Gates were drawn using stained mock-immunized and unstained controls.

Analysis of lung proteome

CD-1 Mice were infected with WT (n=5 or ΔCbpD as described under murine model of intratracheal (IT) PA infection. Uninfected mice (injected with 1× PBS) served as a mock control (CT). Lungs were collected 24 h post IT and homogenized using a Mini BeadBeater and homogenization buffer consisting of 0.25 M NaCl (Sigma), 1% sodium dodecyl sulfate (SDS, Fisher), 1 mM phenylmethylsulfonyl fluoride (PMSF, Sigma), 1× Complete Mini EDTA-free protease and phosphatase inhibitor. Insoluble debris was then pelleted by centrifugation for 15 min at 16000 × *g* and supernatants were transferred to new tubes. Protein concentrations were quantified using Bradford approach and 50 µg of protein extract was dissolved in 6% SDS and 100 mM TEAB to a final volume of 24 µl. Samples were sonicated for 25 cycles (1 min on, 30 sec off) with 100% amplitude in a cuphorn sonicator with watercooler (cuphorn/watercooler: Qsonica. Sonicator: Fisherbrand FB705 sonicator, Fisher). Proteins were reduced with DTT (20 mM) followed by iodoacetamide (40 mM) treatment. Protein digestion and peptide purification were done using an S-trap micro column from protifi (https://protifi.com/pages/protocols) per manufacturer's protocol, with the following modifications: samples were reloaded onto the column after first spin-through; the number of washes after sample binding was increased to 6; digestion was performed with a mix of 2.5 µg trypsin (Promega) and 0.5 µg Lys-C (Wako) in 40 µl of 50 mM TEAB at 37 °C overnight in a humidity chamber.

Peptides were labeled with TMT using the TMT10plex™ Isobaric Label Reagent Set (Thermo scientific) per manufacturer's instructions. A bridge sample containing 5 µg of each sample was TMT 126 labeled. This sample was included in all TMT10plex. Mixing of samples was checked by analyzing 2 µl of a mix of TMT labeled peptides in the mass spec and the ratios used to mix the TMT tagged peptides correctly. Samples were first fractionated by high salt-reverse phase chromatography (7) using an Ultimate 3000 offline HPLC. Next, 100 µg of peptides were reconstituted in 200 mM ammonium formate, pH 10.0 and loaded onto an RP column (Waters Acquity UPLC® BEH C18 1.7 µm 2.1 x 100 mm column). Samples were fractionated using a linear gradient of 0-60% B (90% ACN, 20 mM ammonium formate, pH 10.0) at 150 µl/min for 30 min. Twenty fractions were collected and pooled into 10 fractions using the mixing strategy Fr1 + Fr11, Fr 2 + Fr12, etc. Fractions were frozen at – 80°C. Samples were subsequently dried in a speedvac and reconstituted in 0.1% formic acid.

Peptides were fractionated using a 2-80% acetonitrile gradient in 0.1% formic acid over 140 min at a flow rate of 300 nl/min. The separated peptides were analyzed using a Thermo Scientific Orbitrap Exploris 480 mass spectrometer. MS1 data were collected at 60k resolution over an m/z range at 375-1575 using a maximum injection time of 50 ms. MS data were collected at 45K resolution at maximum injection time 86 ms.

Raw data were analyzed using MaxQuant (version 1.6.17.0) with the integrated Andromeda search engine. MS/MS data were searched against the Uniprot *Mus musculus* (2021) and *P. aeruginosa* database. Perseus (version 1.6.10.43) was used for statistical analysis. The *p*-values were adjusted by applying Benjamini-Hochberg correction with an FDR of 0.01. The π scores or protein significant scores were calculated by taking into consideration both *P* value and fold change as described previously (8). The cut-off values for significance were set to π scores ≥ 2 (α ≤ 0.01). To control for differential protein loading within a TMT ten-plex, the summed protein quantities were adjusted to be equal within a ten-plex as described previously (9). Data was converted to $\log_2$ format, and the bridge channel protein quantity was subtracted from each sample quantity to create a ratio to the bridge. Bridge protein quantity was subtracted from each sample. Bridge sample, now 0, was removed and within each ten-plex, the mean protein expression was centered at 0. Enrichment analysis

was performed using Metascape (release 3.5, August 2021) with minimum overlap, *P* value cut-off, and minimum enrichment set at 3, 0.01, and 2, respectively (10). The STRING database (version 11.5) was utilized to visualize the interaction networks (11). Morpheus was utilized for similarity clustering analysis (https://software.broadinstitute.org/morpheus/).

X-ray crystallography of CbpD catalytic domain

The PA CbpD LPMO (AA10, residues 26-207) was crystallized in 24 well VDE crystallization plates (Hampton Research) using the sitting-drop vapor-diffusion technique. Diffraction-quality crystals grew over several months at 20 °C from a 1:1 (2 µL: 2 µL) mixture of protein (18 mg/mL in 150 mM NaCl, 15 mM Tris-HCl pH 7.5) and reservoir solution containing 0.2 M ammonium chloride and 20% PEG 3350. After flash-cooling in liquid nitrogen, diffraction data were collected at the BioMAX beamline (12) at MAX-IV Laboratory in Lund, Sweden, which was equipped with an EIGER 16M hybrid pixel detector (13). The best crystal diffracted to sub-atomic resolution, challenging the technical limitations imposed by the beamline hardware: at a wavelength of 0.6526 Å, X-ray data could be recorded to 0.75 Å at the detector edge. To increase multiplicity, 4 data sets were collected at 100 K on the same crystal, each covering 360° with 0.1° oscillations. A helical data collection strategy was adopted to spread radiation damage over a larger crystal volume. To achieve full completeness, 2 of the 4 data sets were collected after a 90° rotation around the κ axis. Diffraction data were subsequently integrated and scaled with *XDS* and *XSCALE* from the XDS software package (14), omitting diffraction images with lower diffraction quality, and keeping Friedel pairs separate in merging statistics. Finally, X-ray data were merged and truncated with *AIMLESS* (15) from the *CCP4* program suite (16). Data collection statistics are reported in **Table S1**.

The crystal structure was solved by molecular replacement using the *CCP4* (16) program *PHASER* (17) and a search model generated from the crystal structure of AA10 LPMO from *Tectaria macrodonta* (PDB ID: 6IF7 (18), resolution: 2.2 Å). This structure was identified as the ortholog with highest sequence identity to PaCbpD-domain 1 (52%) by a BLAST (19) search restricted to the Protein Data Bank (PDB) records (https://www.rcsb.org/, (20)). Note that at the time, the 3 Å crystal structure of CbpD (PDB ID: 7SQX (21)). was not yet published. Non-conserved residues were pruned to the gamma atoms with the *CHAINSAW* utility (22) from the *CCP4* program suite (16). The model derived from molecular replacement was gradually improved, alternating between real-space refinement cycles using *Coot* (23) and least-square refinement with *SHELXL* (24), using data to 1.2 Å (**Table S2**). Missing parts of the protein main chain and side chains were added when possible. Subsequently, water molecules were added, based on compatible electron density and matching hydrogen-bonding in the surrounding environment. In later cycles, alternative side chain conformations were modeled, and their occupancy refined with *PHENIX.refine* (25). Toward the end of the refinement process, diffraction data to 0.75 Å were included, carrying out full anisotropic refinement for both the protein and the solvent molecules. During the last cycle, hydrogen atoms were added to all the protein atoms, omitting the hydroxyl hydrogens on Tyr, Thr, Ser and the hydrogens on the protonatable groups of Arg, Lys, Asp and Glu. Additionally, we omitted all the hydrogen atoms on the imidazole ring of the His side chain, to eliminate bias in the assignment of the protonation state. The final model is deposited in the PDB with PDB ID: 8C5N, and the refinement process is summarized in **Table S2**.

Modeling the protonation state of CbpD catalytic domain (AA10)

The coordinates of the LPMO domain of CbpD were processed with the utility *PDBSET* from the *CCP4* (16) software suite. After removing hydrogen atoms, alternative conformations, and anisotropic *B*-factors, the coordinates were used as an input for H++ 3.0 (http://biophysics.cs.vt.edu/hppdetails.php; (26), which is a collection of utilities to prepare a protein structure for a molecular dynamic simulation using the AMBER ff14SB force field (27, 28), calculating the correct state of all the protonable groups. The service was run with all the water molecules included during the refinement process, modeled according to the 3-charge, 4-point rigid water model (OPC) description (29), setting the salinity to 0.15 M, the internal dielectric constant to 10 $F \cdot m^{-1}$ and the external dielectric constant to 80 $F \cdot m^{-1}$. Different pH values relevant for the enzymatic activity were investigated (pH 5.0, 6.2, 6.7, 7.3).

Epitope prediction

The potential discontinuous and continuous CbpD B-cell epitopes were predicted with the Discotope 2.0 server (https://services.healthtech.dtu.dk/service.php?DiscoTope-2.0) (30), using a full-length structural model generated by Alphafold2 as input (UCBPP-PA14 CbpD variant; Uniprot ID: Q02I11, obtained from the Alphafold protein structure database), and default parameters (i.e. -3.7 as threshold for epitope identification). Results were visualized using PyMOL version 2.4.1. (Schrödinger, L.L.C.).

Statistical analysis

Data were analyzed and plotted using GraphPad Prism (version 9) and presented as the mean± standard error of the mean (SEM) unless otherwise indicated in the Materials and Methods section or in the figure legends. If not otherwise specified (*e.g.*, proteomics data), *t*-test, two-way ANOVA, or log-rank test in the GraphPad Prism software package (version 9) were used to identify the statistical significance ($P < 0.05$). Details are given in the figure legends. The statistical analysis related to proteomics data is described under section “Analysis of lung proteome”.

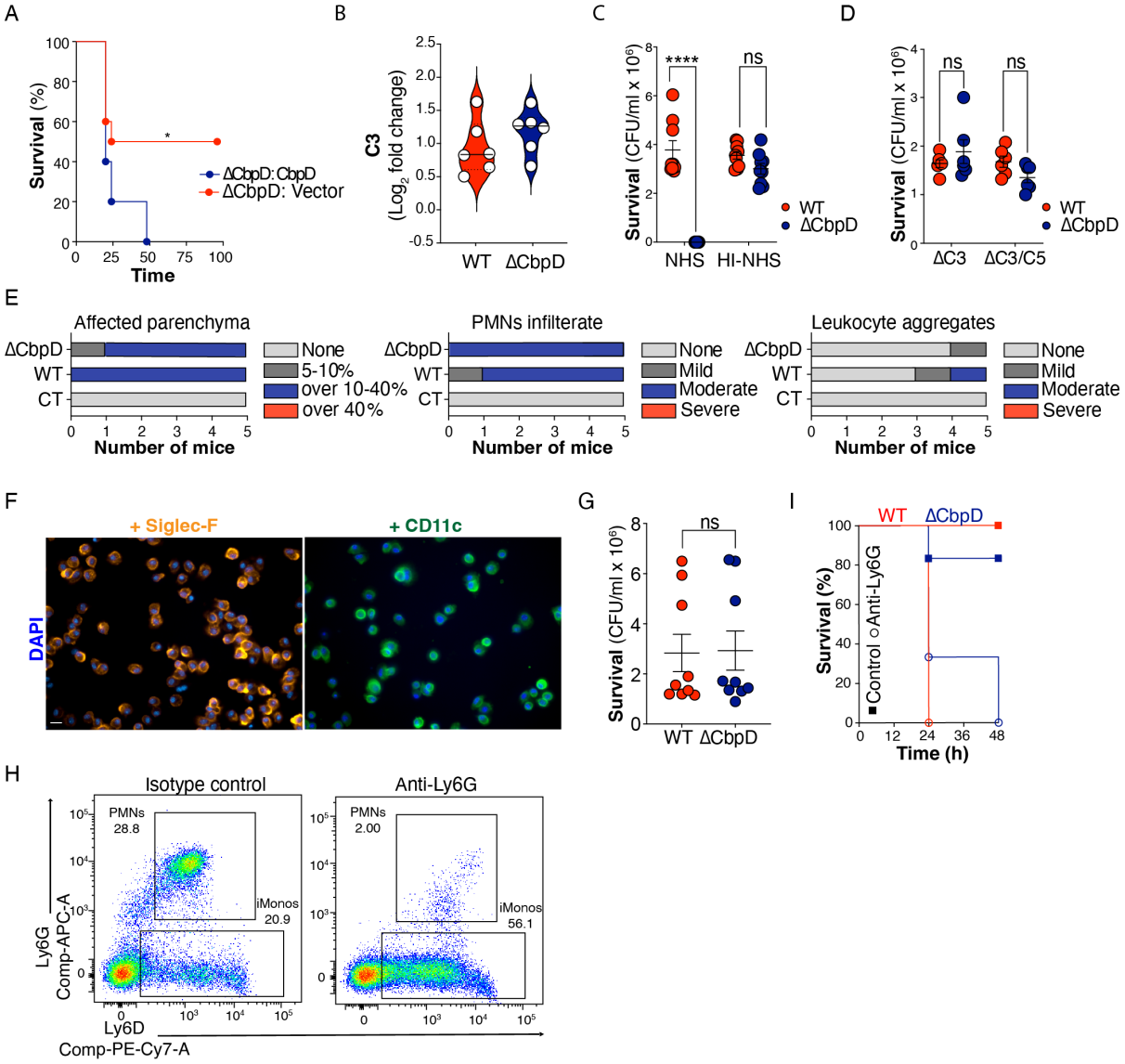

Fig. S1. CbpD-mediated immune responses in the lung during PA infection. (A) CD-1 mice were inoculated intratracheally with 2 × 10^6 CFU/mouse trans-complemented constructs including ΔCbpD:CbpD or ΔCbpD:CbpD (10 mice/group). Survival is represented by Kaplan–Meier survival curves and was analyzed by log-rank (Mantel–Cox) test. *P* = 0.030. **(B)** The mean fold change values of complement C3 in the lung proteome of ΔCbpD- and WT-infected compared to mock-infected (control) mice (5 mice/group; one mouse sample/treatment was utilized as technichal replicate in each TMT group). The data are plotted as the mean (log_2 fold change) ± SEM, representing five biological replicates and analyzed by two-tailed *t*-test. **(C)** Survival of PA WT and ΔCbpD upon incubation for 1h in pooled normal human serum (NHS; 10% v/v) or heat-inactivated serum (HI; 10% v/v) for 1 h. The data are plotted as the mean ± SEM, representing three experiments performed in triplicate. Data are analyzed by two-way ANOVA (Šídák's multiple comparisons test). NHS: *P* = < 0.0001, HI-NHS: *P* = 0.1931. **(D)** Survival of PA WT and ΔCbpD upon incubation in ΔC3 and ΔΔC3C5 human serum (10%) for 1 h. The data are plotted as the mean ± SEM, representing two experiments performed in triplicate. Data were analyzed by two-way ANOVA (Šídák's multiple comparisons test). **(E)** Hematoxylin and eosin-stained sections of spleen tissues from infected (WT or ΔCbpD) and uninfected CD-1 mice (n = 5 mice/group) collected 24 h post IT infection and analyzed by light microscopy (Fig. 1I). The histopathological scoring analysis of neutrophil infiltration, leukocyte aggregates and affected parenchyma of the lung tissue is shown as a histogram. **(F)** Representative fluorescence microscopy images of Siglec F and CD11c expression in pooled murine alveolar macrophage (n = 5 CD-1 female mice). The markers were detected by PE rat anti-mouse Siglec F and FITC hamster anti-mouse CD11c. Cell nuclei were stained with DAPI. Two separate channels were merged into a single image by Fiji. The scale bar represents 10 µm. The imaging was performed once in duplicate. **(G)** Survival of PA WT

and ΔCbpD upon incubation for 1.5 h with pooled alveolar macrophages that were obtained from bronchoalveolar lavage (BAL) of ten-week-old CD-1 mice (n = 5 mice/experiment). The data are plotted as the mean ± SEM, representing two experiments performed at least in triplicate. Data are analyzed by two tailed *t*-tests. **(H)** Representative flow plots of splenic neutrophils. Eight-week-old CD-1 mice were intraperitoneally injected with 100 µg anti-Ly6G (clone 1A8) or isotype control (clone 2A3). Spleens from depleted (n = 3) and control mice (n = 3) were harvested 24 h post-injection to confirm depletion and processed for flow cytometry. Neutrophils were gated for cells, singlets, live, $CD11b^+$, Ly-6C, Ly-6G. The gating strategy is described in Fig. S4. **(I)** CD-1 mice (n=6 mice/group) were treated intraperitoneally with anti-Ly6G or isotype control to deplete neutrophils (as for Fig. S1I). 24 h post-depletion, mice were inoculated intratracheally with 0.1×10^6 CFU PA WT or ΔCbpD per mouse. Data were analyzed by log-rank (Mantel–Cox) test and survival is represented by Kaplan–Meier survival curves.

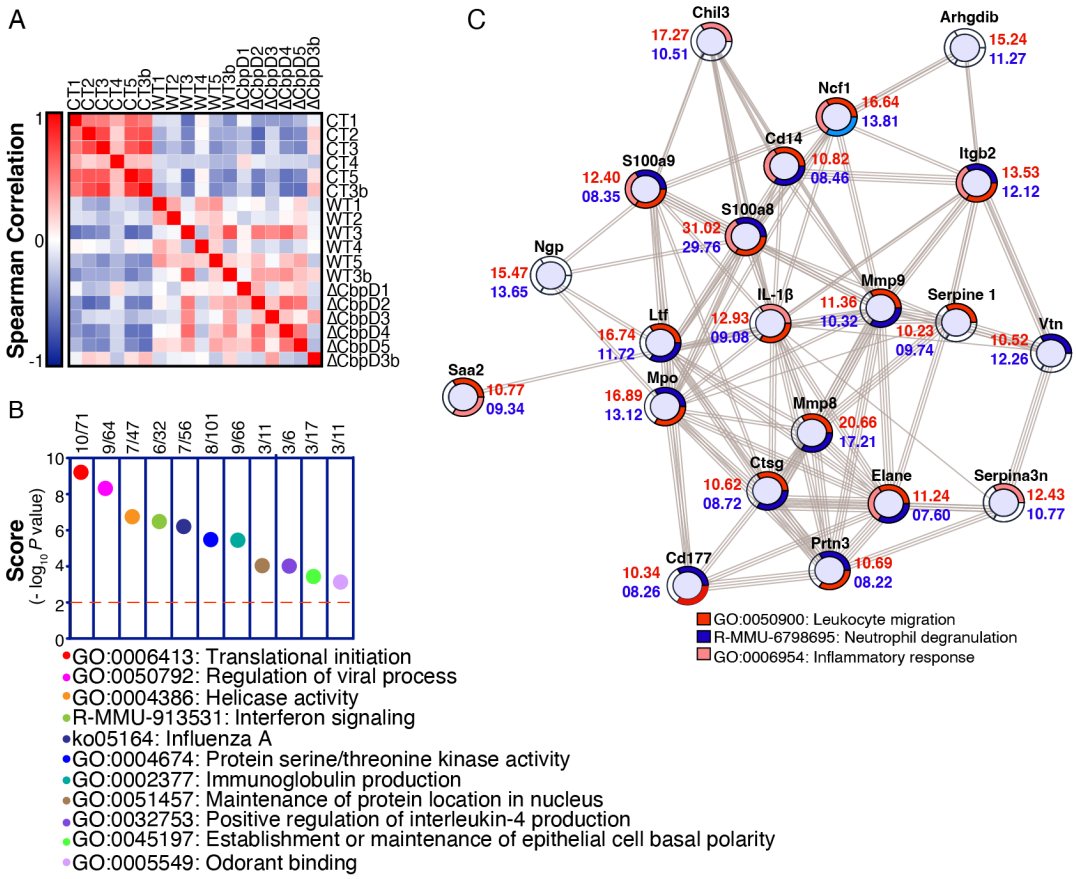

Fig. S2. The effect of PA on the lung proteome during intratracheal infection *in vivo*. (A) Similarity clustering of lung proteome in WT-, ΔCbpD- and mock (CT)- infected mice was analyzed with Morpheus. Each square represents one biological replicate (5 mice/group; one mouse sample per treatment was utilized as a technical replicate for each TMT group). **(B)** Dot plot of enrichment score ($-\log_{10} P$ value ≥ 2) showing pathways and cellular processes that were enriched in the lung proteome (Dataset 4) of WT-infected mice. Enrichment analysis was performed using the list of upregulated proteins belong to the unique category by Metascape and the *P* value was calculated based on the cumulative hypergeometric distribution. **(C)** STRING network analysis showing connection of the top shared regulated proteins (π score ≥ 10 at least in one group) in the lung proteome of WT- and/or ΔCbpD-infected mice vs control (Dataset 3). The π score values are depicted next to the nodes in red (WT) and blue (ΔCbpD). Proteins without any interaction partners within the network (singletons) are omitted from the visualization.

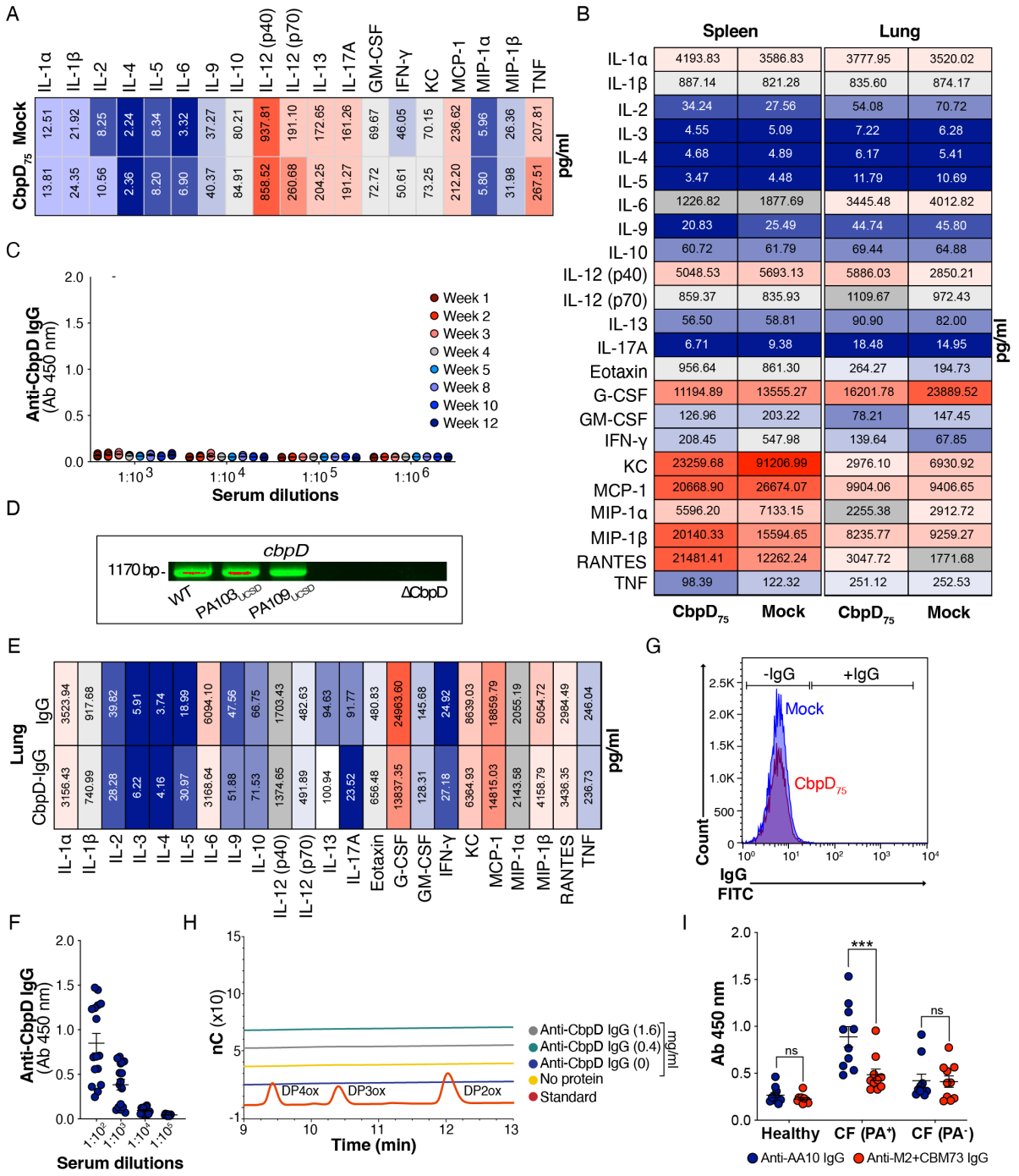

Fig. S3. Immunization with CbpD *in vivo*. **(A)** The categorical heatmap shows the concentration of cytokines and chemokines in the serum of $CbpD_{75}$ (n=24 mice)- and mock (n = 9 mice)- immunized CD-1 mice at day 20 postprime. The samples were examined using Bio-Plex Pro™ mouse cytokine assay. Data depict the geometric mean of the cytokine values. The data were analyzed by multiple unpaired *t*-test and the FDR-adjusted *P* value (or *q* value) was determined using the two-stage step-up method of Benjamini, Krieger and Yekutieli. **(B)** The categorical heatmap shows the concentration of cytokines and chemokines in the lung and spleen homogenates of $CbpD_{75}$- and mock-immunized CD-1 mice that were intratracheally (as described in Fig. 3E) and intravenously (as described in Fig. 3F) challenged with WT PA, respectively. The samples were examined using Bio-Plex Pro™ mouse cytokine assay. Data depict the geometric mean of the cytokine values. The data were analyzed by multiple unpaired *t*-test and the FDR-adjusted *P* value (or *q* value) was determined using the two-stage step-up method of Benjamini, Krieger and Yekutieli. **(C)** Dynamics of changes in the titers of CbpD-IgG in mock-immunized CD-1 murine sera in the period from 1 to 12 weeks postprime. The timeline of the

immunization is described in Fig. 3A. CbpD-IgG titers in the CbpD-immunized group are shown in Fig. 3G. The data are plotted as the mean ± SEM, representing 5 mice per group. **(D)** Agarose gel electrophoresis showing PCR-amplified *cbpD* in the genomic DNA of PA clinical isolates $PA103_{UCSD}$ and $PA109_{UCSD}$, which was recovered from cystic fibrosis patients. The uncropped agarose gel is shown in Fig. S6. **(E)** The categorical heatmap shows the concentration of cytokines and chemokines in the lung homogenates of anti-CbpD IgG- (70 µg/mouse, n = 7 mice) and IgG-treated (70 µg/mouse, n = 9 mice) (intravenously) naïve CD-1 mice. The recipient mice were intratracheally challenged with $1x10^6$ CFU/mouse WT PA 16 h post adoptive transfer of antibodies. The lungs were collected 24 h post infection for cytokine analysis using Bio-Plex Pro™ mouse cytokine assay. Data depict the geometric mean of the cytokine values. The data were analyzed by multiple unpaired *t*-test and the FDR-adjusted *P* value (or *q* value) was determined using the two-stage step-up method of Benjamini, Krieger and Yekutieli. **(F)** Total serum anti-CbpD IgG in healthy human individuals. The data are plotted as the mean ± SEM, representing 16 individuals. **(G)** Representative histogram of mouse IgG from CbpD- (red, $CbpD_{75}$ regimen, n=5 mice) and mock-immunized (blue, n = 5 mice) serum (5%) bound to PA analyzed by flow cytometry using Alexa Fluor™ 488 conjugated rabbit anti-mouse IgG. **(H)** HPLC analysis of reaction products emerging from a mixture of copper-saturated recombinant CbpD, β-chitin, and mouse anti-CbpD IgG, in buffer (20 mM Tris-HCl pH 7.0), for 3 h at 37 °C under shaking. The degrees of polymerization (DP) of chitooligosaccharide aldonic acids in a standard sample are depicted. The reactions with the 1 mM ascorbate as reducing agent, which resulted in oxidized product generation, are shown in Fig. 5G for comparison. **(I)** Total plasma anti-AA10 and anti-M2+CBM73 IgG in healthy human individuals and cystic fibrosis (CF) patients (dilution $1:10^3$). CF patients were colonized (PA^+) or non-colonized (PA^-) with *PA* at the time of blood collection. The data are plotted as the mean ± SEM of two independent ELISA experiments, representing 5 individuals per group. Data were analyzed by two-way ANOVA (Šídák's multiple comparisons test). AA10 vs Mx+CBM73 (CF (PA^+)): $P = 0.0001$. Each data point represents an individual mouse/human, and the significant differences are marked with asterisks (*): $*P \leq 0.05$; $**P \leq 0.01$; $***P \leq 0.001$; $****P \leq 0.0001$.

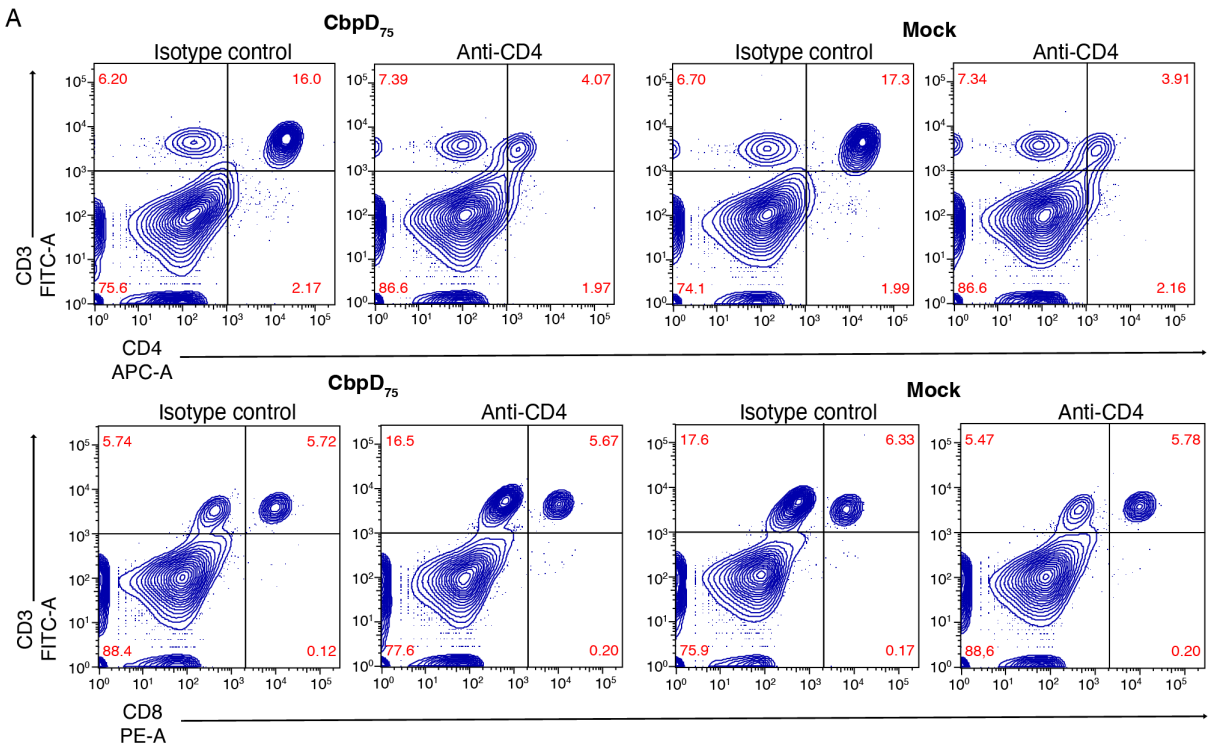

Fig. S4. Depletion of CD4 cells in CbpD-immunized mice. (A) Representative flow plots of splenic CD4 cells. Mice were intravenously injected with 300 µg/mouse ultra-LEAF anti-CD4 (clone GK1.5) or isotype control 48 h and 24 h prior to infection. Spleens from depleted (n = 2) and control mice (n = 2) were harvested 24 h post adoptive transfer of the second dose to confirm depletion and processed for flow cytometry. Splenocytes were gated for cells, singlets, live, $CD3^+$, $CD4^+$, and $CD8^+$.

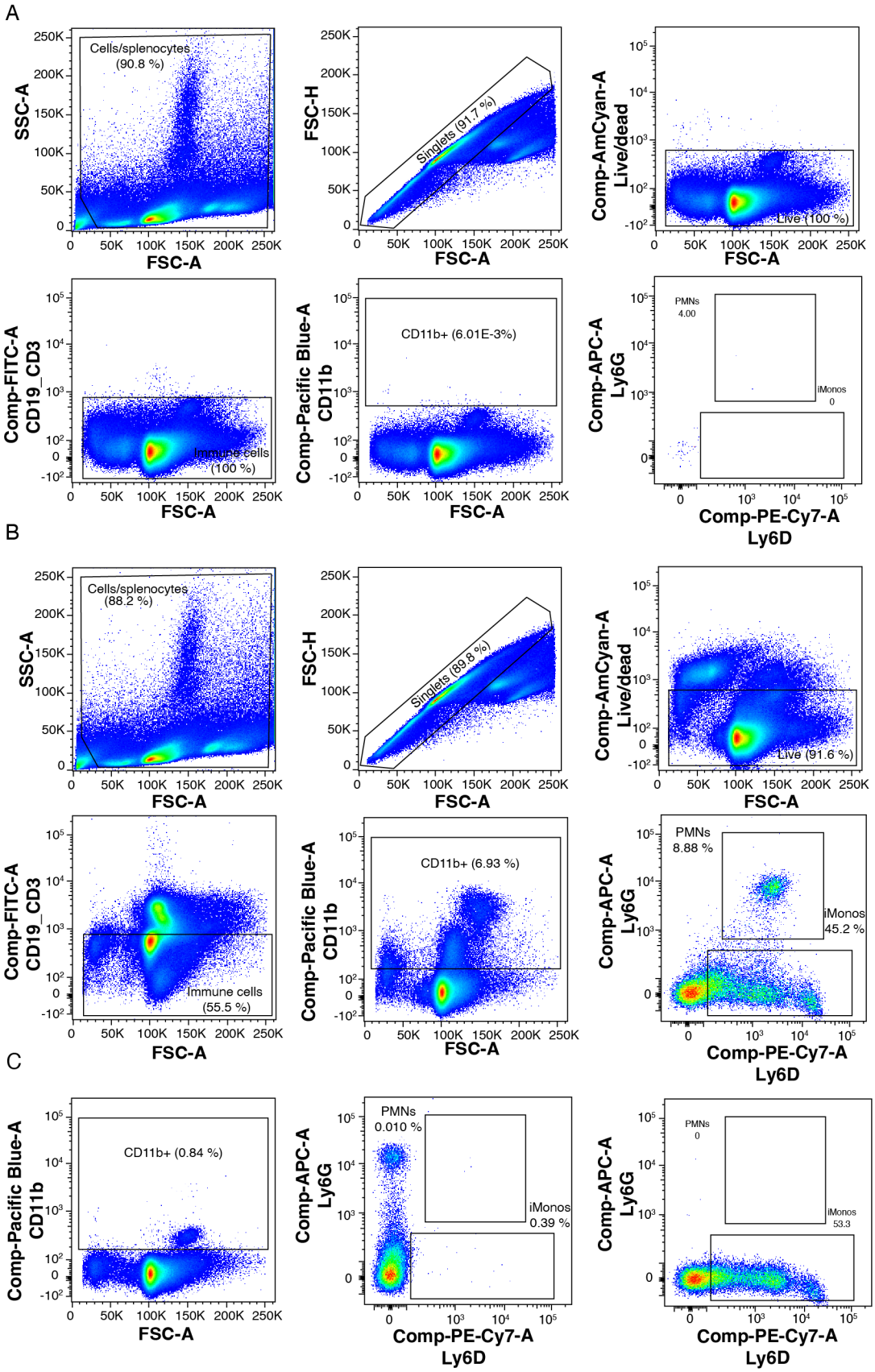

Fig. S5. Gating strategy. The representative flow plots demonstrate an example of gating strategy used for multicolor flow cytometric data to identify the viable immune cells in splenocytes (Figs. S1H and S4). The data were analyzed with FlowJo and splenocytes were gated on SSC versus FCS for cells. Next, the cells were gated for singlet, live cells, and multiple markers of the immune cells that

were conjugated to different fluorochromes. The flow plots are provided for **(A)** unstained, **(B)** stained, and when applicable **(C)** fluorescence minus one (FMO) control.

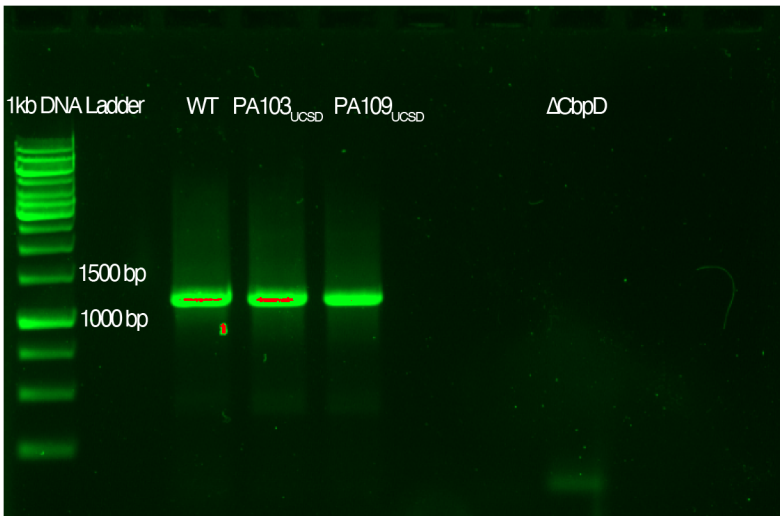

Fig. S6. PCR-amplified product of *cbpD* in the genomic DNA of PA109$_{UCSD}$ and PA103$_{UCSD}$. PA WT and ΔCbpD served as positive and negative controls, respectively. The agarose gel represents the uncropped image corresponding to Fig. S3D.

Table S1. X-ray data collection and refinement statistics for CbpD LPMO domain

X-ray source	MAX-IV Laboratory - BioMAX
Wavelength, Å	0.6526
Space group	$P2_1$
Unit cell parameters – a,b,c (Å), β (°)	31.6, 54.6, 48.0, 99.3
Resolution (Å)	47.4-0.75 (0.76-0.75)
Mean I/σ(I)	23.5 (0.6)
No. of unique reflections	198464 (7613)
Multiplicity	19.9 (8.3)
Completeness (%)	97.0 (76.0)
$CC_{1/2}$ (%)	99.9 (30.0)
R_{merge} (within I+/I-) (%)	5.3 (>100)
R_{merge} (all I+ and I-) (%)	5.5 (>100)
R_{meas} (within I+/I-) (%)	5.6 (>100)
R_{meas} (all I+ and I-) (%)	5.6 (>100)
R_{pim} (within I+/I-) (%)	1.7 (>100)
R_{pim} (all I+ and I-) (%)	1.2 (>100)
Wilson B-factor (Å^2)	6.9
Refinement	
Resolution range (Å)	47.4-0.75
R_{work}/R_{free} (%)	14.0/15.2
Average B-factors (Å^2)	
protein	9.3
ligands	9.9
solvent	17.5
Number protein chains in the a.s.u.	1
Number of non-hydrogen atoms	
Protein	1607
Water	161
r.m.s.d. from ideal geometry	
Bond lengths (Å)	0.02
Bond angles (deg.)	2.0
Ramachandran plot	
Favoured (%)	99.5
Allowed (%)	0.5
Outliers (%)	0.0
PDB deposition code	8C5N

Table S2. Refinement cycles and extension of resolution

Cycle No.	**Software**	**Res. (Å)**	**Action**	R_{work}/R_{free} *(%)*
1	SHELXL	1.2	Isotropic refinement on the MR result	25.3/27.5
2	SHELXL	1.2	model adjustments, isotropic refinement	20.0/21.8
3	SHELXL	1.2	model adjustments, added water, isotropic refinement,	18.2/19.8
4	PHENIX.refine	1.2	occupancy refinement, anisotropic refinement	14.1/15.6
5	SHELXL	1.2	model adjustments, isotropic refinement	17.2/19.8
6	SHELXL	1.2	model adjustments, isotropic refinement	17.6/19.7
7	SHELXL	0.9	model adjustments, isotropic refinement, extended the resolution to 0.9 Å	19.0/20.4
8	SHELXL	0.9	model adjustments, isotropic refinement	19.1/20.5
9	PHENIX.refine	0.9	occupancy refinement, anisotropic refinement	17.0/17.5
10	SHELXL	0.9	model adjustments, isotropic refinement	19.0/20.4
11	SHELXL	0.9	anisotropic refinement	13.8/15.7
12	SHELXL	0.79	model adjustments, resolution extended to 0.79 Å, refinement	13.9/15.7
13	SHELXL	0.75	model adjustments, resolution extended to 0.75 Å, anisotropic refinement	13.6/14.7
14	PHENIX.refine	0.75	model adjustments, occupancy refinement, anisotropic refinement	15.7/16.2
15	SHELXL	0.75	anisotropic refinement	14.6/15.9
16	SHELXL	0.75	Included hydrogens, anisotropic refinement (except hydrogens)	14.0/15.2

SI References

1. L. G. Rahme, *et al.*, Common virulence factors for bacterial pathogenicity in plants and animals. *Science* **268**, 1899–1902 (1995).
2. F. Delvillani, *et al.*, Tet-Trap, a genetic approach to the identification of bacterial RNA thermometers: application to *Pseudomonas aeruginosa*. *RNA* **20**, 1963–1976 (2014).
3. F. Askarian, *et al.*, The lytic polysaccharide monooxygenase CbpD promotes *Pseudomonas aeruginosa* virulence in systemic infection. *Nat. Commun.* **12**, 1230 (2021).
4. D. K. Nayak, O. Mendez, S. Bowen, T. Mohanakumar, Isolation and in Vitro culture of murine and human alveolar macrophages. *J. Vis. Exp.* (2018) https:/doi.org/10.3791/57287.
5. G. Boivin, *et al.*, Durable and controlled depletion of neutrophils in mice. *Nat. Commun.* **11**, 2762 (2020).
6. P. Santos-Moriano, *et al.*, Enzymatic production of fully deacetylated chitooligosaccharides and their neuroprotective and anti-inflammatory properties. *Biocatalysis and Biotransformation* **36**, 57–67 (2018).
7. D. R. Stein, *et al.*, High pH reversed-phase chromatography as a superior fractionation scheme compared to off-gel isoelectric focusing for complex proteome analysis. *Proteomics* **13**, 2956–2966 (2013).
8. Y. Xiao, *et al.*, A novel significance score for gene selection and ranking. *Bioinformatics* **30**, 801–807 (2014).
9. D. P. Nusinow, *et al.*, Quantitative proteomics of the cancer cell line encyclopedia. *Cell* **180**, 387-402.e16 (2020).
10. Y. Zhou, *et al.*, Metascape provides a biologist-oriented resource for the analysis of systems-level datasets. *Nat. Commun.* **10**, 1523 (2019).
11. D. Szklarczyk, *et al.*, The STRING database in 2021: customizable protein-protein networks, and functional characterization of user-uploaded gene/measurement sets. *Nucleic Acids Res.* **49**, D605–D612 (2021).
12. T. Ursby, *et al.*, BioMAX - the first macromolecular crystallography beamline at MAX IV Laboratory. *J. Synchrotron Radiat.* **27**, 1415–1429 (2020).
13. A. Casanas, *et al.*, EIGER detector: application in macromolecular crystallography. *Acta Crystallogr D Struct Biol* **72**, 1036–1048 (2016).
14. W. Kabsch, *XDS*. *Acta Crystallographica Section D Biological Crystallography* **66**, 125–132 (2010).
15. P. R. Evans, G. N. Murshudov, How good are my data and what is the resolution? *Acta Crystallogr. D Biol. Crystallogr.* **69**, 1204–1214 (2013).
16. M. D. Winn, *et al.*, Overview of the *CCP4* suite and current developments. *Acta Crystallogr. D Biol. Crystallogr.* **67**, 235–242 (2011).
17. A. J. McCoy, *et al.*, *Phaser* crystallographic software. *J. Appl. Crystallogr.* **40**, 658–674 (2007).
18. S. K. Yadav, Archana, R. Singh, P. K. Singh, P. G. Vasudev, Insecticidal fern protein Tma12 is possibly a lytic polysaccharide monooxygenase. *Planta* **249**, 1987–1996 (2019).
19. E. W. Sayers, *et al.*, Database resources of the national center for biotechnology information. *Nucleic Acids Res.* **50**, D20–D26 (2022).
20. H. M. Berman, *et al.*, The Protein Data Bank. *Acta Crystallogr. D Biol. Crystallogr.* **58**, 899–907 (2002).
21. C. M. Dade, *et al.*, The crystal structure of CbpD clarifies substrate-specificity motifs in chitin-active lytic polysaccharide monooxygenases. *Acta Crystallogr D Struct Biol* **78**, 1064–1078 (2022).
22. N. Stein, *CHAINSAW*: A program for mutating pdb files used as templates in molecular replacement. *Journal of Applied Crystallography* **41**, 641–643 (2008).
23. P. Emsley, B. Lohkamp, W. G. Scott, K. Cowtan, Features and development of *Coot*. *Acta Crystallogr. D Biol. Crystallogr.* **66**, 486–501 (2010).
24. G. M. Sheldrick, Crystal structure refinement with *SHELXL*. *Acta Crystallogr. B* **71**, 3–8 (2015).
25. P. V. Afonine, *et al.*, Towards automated crystallographic structure refinement with *PHENIX.refine*. *Acta Crystallogr. D Biol. Crystallogr.* **68**, 352–367 (2012).
26. R. Anandakrishnan, B. Aguilar, A. V. Onufriev, H++ 3.0: automating p*K* prediction and the preparation of biomolecular structures for atomistic molecular modeling and simulations. *Nucleic Acids Res.* **40**, W537-41 (2012).
27. C. Tian, *et al.*, ff19SB: amino-acid-specific protein backbone parameters trained against quantum mechanics energy surfaces in solution. *J. Chem. Theory Comput.* **16**, 528–552 (2020).
28. J. A. Maier, *et al.*, ff14SB: improving the accuracy of protein side chain and backbone parameters from ff99SB. *J. Chem. Theory Comput.* **11**, 3696–3713 (2015).
29. S. Izadi, R. Anandakrishnan, A. V. Onufriev, Building water models: a different approach. *J. Phys.*

Chem. Lett. **5**, 3863–3871 (2014).
30. J. V. Kringelum, C. Lundegaard, O. Lund, M. Nielsen, Reliable B cell epitope predictions: impacts of method development and improved benchmarking. *PLoS Comput. Biol.* **8**, e1002829 (2012).

Description of Additional Supplemental Files

File Name: Dataset 1
Description: Lung proteome of WT (PA14), ΔCbpD- and mock-infected mice (n=5 mice/group). Data were analyzed by tandem mass tag (TMT)-based quantitative proteomics.

File Name: Dataset 2
Description: List of regulated proteins identified by comparing the WT- and ΔCbpD- infected versus mock-infected mice (Control) lung proteomes. Cut-off values were ranked by significance and fold change using π value ≥ 2.

File Name: Dataset 3
Description: List of regulated proteins (π value ≥ 2) that were commonly regulated (i.e., shared) in WT- and ΔCbpD-infected versus mock-infected (control) lung proteomes. The list covers regulated proteins from Dataset 2.

File Name: Dataset 4
Description: List of dysregulated proteins (π value ≥ 2) that were only regulated (i.e., unique) in WT- or ΔCbpD-infected versus mock-infected (control) proteomes. The list covers regulated proteins from Dataset 2.